Received: 16 June 2021 | Revised: 21 July 2021 | Accepted: 22 July 2021

DOI: 10.1002/pat.5463

SHORT COMMUNICATION

polymers advanced technologies WILEY

Melt electrowriting of poly(vinylidene difluoride) using a heated collector

Juliane C. Kade[1] | Paul F. Otto[1] | Robert Luxenhofer[2,3] | Paul D. Dalton[1,4]

[1]Department of Functional Materials in Medicine and Dentistry and Bavarian Polymer Institute, University Hospital Würzburg, Würzburg, Germany

[2]Polymer Functional Materials, Chair for Advanced Materials Synthesis, Department of Chemistry and Pharmacy, Julius-Maximilians-University Würzburg, Würzburg, Germany

[3]Soft Matter Chemistry, Department Chemistry and Helsinki Institute of Sustainability Science, Faculty of Science, University of Helsinki, Helsinki, Finland

[4]Phil and Penny Knight Campus for Accelerating Scientific Impact, University of Oregon, Eugene, Oregon, USA

Correspondence
Paul D. Dalton, Department of Functional Materials in Medicine and Dentistry and Bavarian Polymer Institute, University Hospital Würzburg, Pleicherwall 2, 97070, Würzburg, Germany.
Email: pdalton@uoregon.edu

Funding information
Joachim Herz Stiftung, Grant/Award Number: Juliane Kade; Volkswagen Foundation, Grant/Award Number: 93418

Abstract

Previous research on the melt electrowriting (MEW) of poly(vinylidene difluoride) (PVDF) resulted in electroactive fibers, however, printing more than five layers is challenging. Here, we investigate the influence of a heated collector to adjust the solidification rate of the PVDF jet so that it adheres sufficiently to each layer. A collector temperature of 110°C is required to improve fiber processing, resulting in a total of 20 fiber layers. For higher temperatures and higher layers, an interesting phenomenon occurred, where the intersection points of the fibers coalesced into periodic spheres of diameter 206 ± 52 μm (26G, 150°C collector temperature, 2000 mm/min, 10 layers in *x*- and *y*-direction).The heated collector is an important component of a MEW printer that allows polymers with a high melting point to be processable with increased layers.

KEYWORDS
additive manufacturing, electroactive, melt electrowriting, polymer processing

1 | INTRODUCTION

Melt electrowriting (MEW) is a high-resolution 3D printing technology that fabricates well-defined structures with fiber diameters down to the sub-micron range.[1,2] The technique offers the production of scaffolds with fibers larger than those processed using solution electrospinning (SES) and smaller than using extrusion-based 3D printing while maintaining the control over the fiber placement. There remains a limited number of polymers that have been processed via MEW, however, this is recently changing.[3] The most commonly used polymer for MEW is poly(ε-caprolactone) (PCL), as it minimally degrades during processing and micrometer-range fibers can be stacked upon each other up to 7 mm in thickness.[4]The MEW processing capabilities for PCL are the current gold standard for the technique.

Another polymer that has been demonstrated compatible with MEW is poly(vinylidene difluoride)(PVDF),[5] an electroactive polymer with a range of applications involving electronic,[6–9] actuating,[10] biomedical materials[11]and membranes.[12–14] One noticeable distinction between MEW processing of PVDF in this study and PCL, is that the printing process becomes unstable above five layers, with warping of the scaffold from the collector back towards the printer head. This limitation in the number of printable layers resulted in thin PVDF samples that were difficult to handle and manipulate.

MEW is, however, a multi-parametric technology and that different variables can be altered to achieve improved printing outcomes, including a final fiber diameter.[15] Other important features include fiber sagging and inter-fiber fusion, as these define the final mechanics of the printed material.

2 | MATERIALS AND METHODS

The white PVDF powder (Piezotech Kynar RC10.287) was used as received,[5] loaded into a 3 ml glass syringe (Fortuna Optima 3 ml Luer

Lock) and connected to an injection cannula (26-gauge with Luer Lock, Carl Roth, Germany) with a cut length of 5.0 ± 0.5 mm. Direct writing was performed on a MEW printer, equipped with a custom-made heated collector as previously described.[16] More details about the printer and the heated collector can be found in the supporting information. The distance between the glass microscope slides (ground edge, cat # 631–1552, VWR, Germany), which are placed and fixed with tape on the collector, was set to 4.0 ± 0.3 mm depending on the collector temperature. The applied potential difference was kept constant and set to 3.0 ± 0.08 kV. The polymer within the syringe, as well as the nozzle tip were heated to 190 ± 5°C and, when used, the collector temperature was varied from 50 to 150°C. For collector temperatures of 100–120°C, the collector distance required adjustments to 3.3 ± 0.3 mm and at 150°C the distance was set to 2.5 ± 0.3 mm. The polymer melt was extruded by applying 3.0 ± 0.1 bar, which enabled direct writing at collector speeds between 1000 and 4000 mm/min.

The surface contact angle of the PVDF scaffolds was investigated with anoptical contact angle measuring and contour analysis system OCA (DataPhysics Instruments GmbH, Germany). A droplet of deionized water (3 μl) was deposited onto the scaffold and the contact angle was calculated using the SCA 20 software (4.4.3 build 1053, DataPhysics Instruments GmbH, Germany). Experiments were repeated for three different locations on each scaffold with three scaffolds per condition. The average contact angle between each side of the droplet and the scaffold surface was then calculated.

SEM imaging of the scaffolds sputter-coated with 4 nm platinum was performed using a Crossbeam 340 (Carl Zeiss Microscopy GmbH, Germany). Videography was conducted using a Nikon Z6 digital camera with a Nikon ED 200 mm lens and video editing was done using the software DaVinci Resolve 16.2.7.01.

3 | RESULTS AND DISCUSSION

This study was directed towards the influence of a heated collector on the layer stacking of PVDF using MEW, specifically towards avoiding the warping of the final printed structure. As previously shown by Florczak et al.,[5] the layer stacking was limited to around five layers in *x*- and *y*-direction. This phenomenon of fiber lifting is illustrated by screenshots in the Figure S1A–C when a nonheated collector at room temperature is used. This lifting and warping of the printed construct can cause jet break-up and introduces defects as fibers get attracted back towards the print head. Warping is also a phenomenon when the extruded material starts to detach from the collector substrate while printing and does then interfere with the printing process.[17] This phenomenon is well-known from FDM printing and can be related to the shrinkage and remaining stresses in the polymer material when extruded from a nozzle.[17]When processing PVDF using MEW, the printed construct first starts to lift at the edges and corners of the scaffold until it quite often gets attracted to the print head completely, most-likely resulting in melting and damage to the printed structure (Figure S1D–F). However, it can also happen that warping does occur without significantly effecting the resulting scaffold outcome.

To overcome this defect, a heated collector was tested at temperatures between 50 and 150°C with the latter indicating the maximum temperature as the fibers lose their shape. Such increasing fiber flattening/melting onto the collector substrate is expected and was observed when processing polypropylene or poly(vinylidene fluoride-co-trifluoroethylene) onto a heated collector with increasing temperature.[16,18] This slightly affected the fiber diameter which ranged from 35 ± 16 to 39 ± 9 μm for RT to 110°C at a printing speed of 4000 mm/min. At collector temperatures of 150°C, the fiber fusion and coalescing were so conspicuous that the diameter was significantly larger with an average diameter of 48 ± 25 μm when using the same printing parameters. The heating of the collector substrate to 120°C enabled both fiber adherence and, post-cooling, sample removal without damage.

SEM images show the fiber morphology from above, side and underneath views indicating fiber fusion and embossing with increasing collector temperature varying from room temperature to 50, 100 and 150°C (Figure 1).

The fabricated constructs in Figure 1 seem to be strongly influenced by the collector temperature as the heat increases the stacking accuracy, as well as the solidification rate of the polymer jet. With increasing collector temperature, starting at 100°C, the fiber showed rougher surfaces due to spherulite formation. Similarly seen with PCL,[19] these spherulites are formed by the slow cooling of the jet. Spherulite formation is expected to affect the alignment of polymer chains along the length of the printed fiber, with implications for beta-phase formation (Figure S2). Without the use of a heated collector, the resulting construct shows no fiber fusion limiting the handling of the construct (Video S1) and therefore, leading to an insufficient design stability. With the usage of a heated collector starting at 50°C, the fabricated constructs show slight fiber fusion (Figure 1).The underneath view of the constructs also shows increasing embossing of the fibers with increasing collector temperature. Figure 2A,B shows how the fiber deposition improves with the collector temperature of 120°C, while Figure 2C shows how warping occurs with such scaffolds printed with the collector at RT.

Scaffolds printed at RT or a collector temperature of 50°C seem to be influenced regarding their stacking accuracy by the printing speed (Figure S3). With increasing printing speed, varied from 1000, 2000 to 4000 mm/min, the scaffolds consist of more straight fibers with enhanced printing precision. The fastest speed significantly improved the layer stacking (supporting information Figure S3).

At collector temperatures of at least 100°C, the lifting of the scaffolds has been reduced compared to room temperature, which might be due to the better adherence and melting of the first fibers printed onto the collector substrate, as indicated by the increasing embossing of the fibers (Figure 1). The heated collector leads to a slower solidification rate of the MEW jet, as well as an increase in the fiber area touching the collector substrate (Figure 1).This change in the jet behavior is also leading to less straight fibers when keeping the collector distance at 4.4 mm, therefore, this gap required adjustments to a

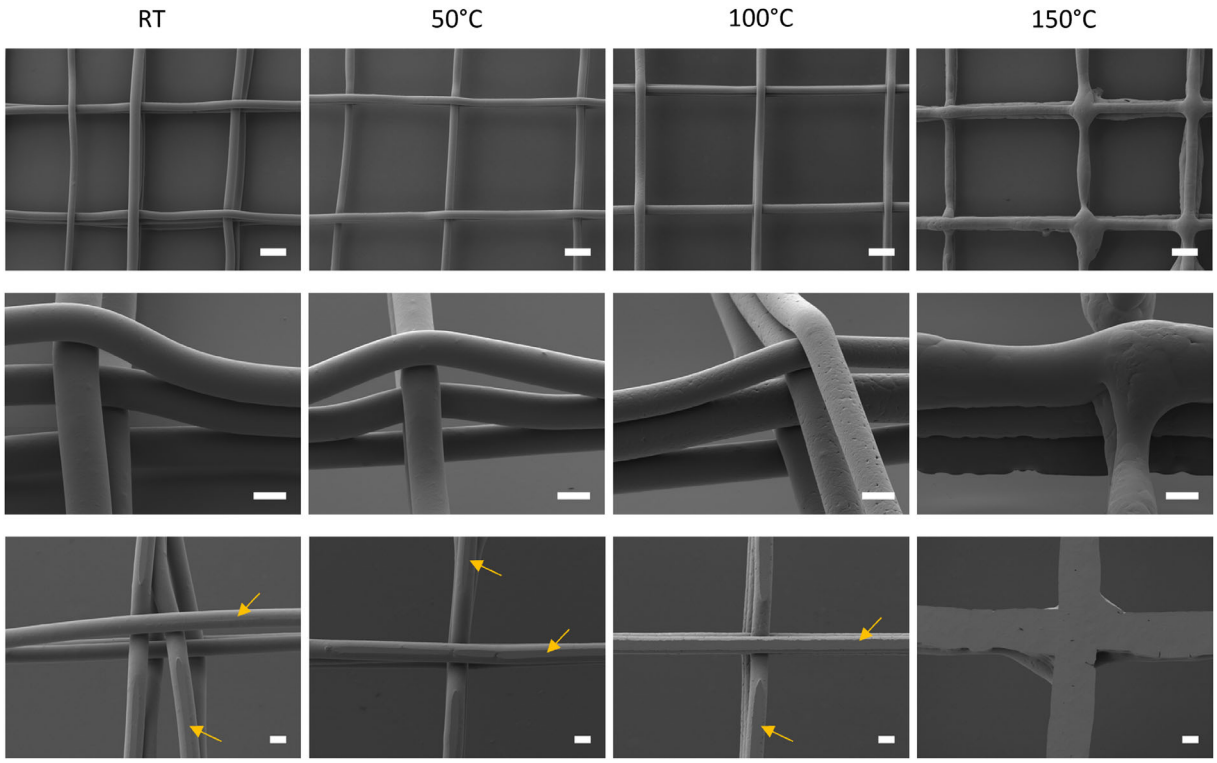

FIGURE 1 SEM images showing scaffolds with three layers in *x*- and *y*-direction printed at 4000 mm/min onto a collector at room temperature, 50, 100 and 150°C showing the above view (first row), tiled/side view (middle row) and underneath view (third row). Yellow arrows indicate the embossing of the fibers onto the collector substrate, Scale bars for the upper, middle and lower row are 100, 25 and 25 μm, respectively

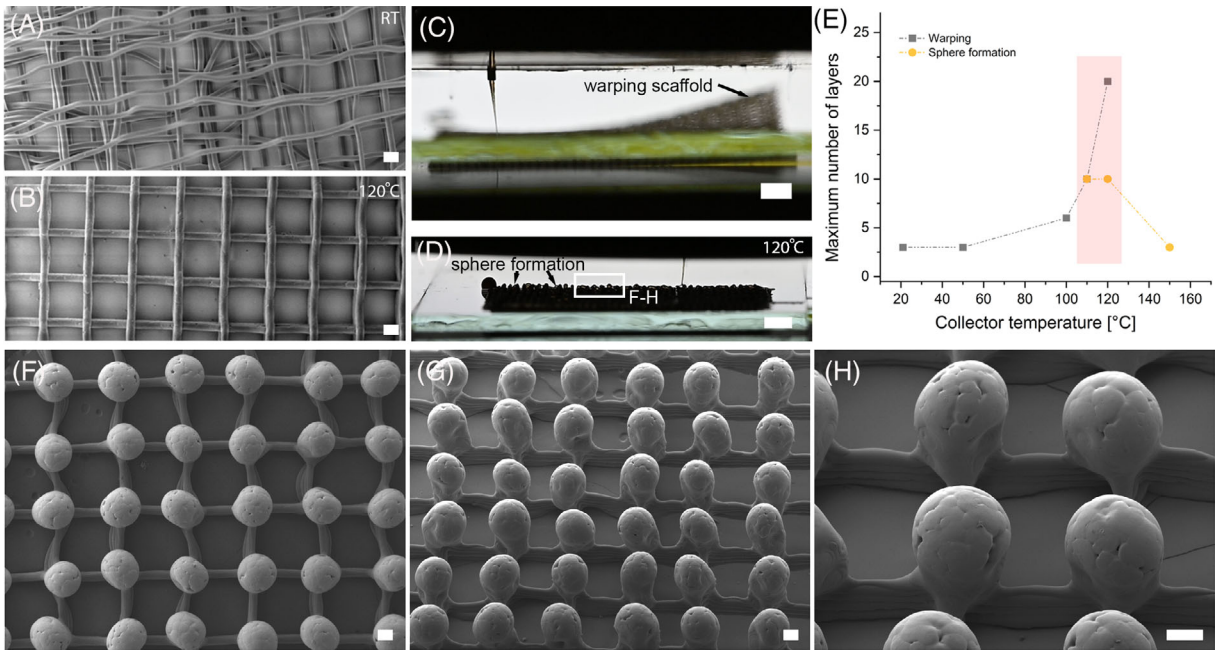

FIGURE 2 Warping and sphere formation for PVDF scaffolds. SEM image of three-fiber layers at (A) RT and (B) 120°C. (C) Photograph of a print at RT that is warping and lifting off the collector. (D) Photograph of thicker samples where spheres can be seen forming with increased layer height. (E) Graphical illustration showing the correlation between the maximum number of layers in *x*- and *y*-direction and the collector temperature. SEM images showing the coalesced spheres on the scaffold printed at 2000 mm/min due to the heat from the print head (F) above view, (G) side view and overview image and (H) magnified side view showing the still existing lower layers and the coalesced spheres. Scale bars = (A,B) 200 μm, (C,D) 2 mm and (F–H) 100 μm

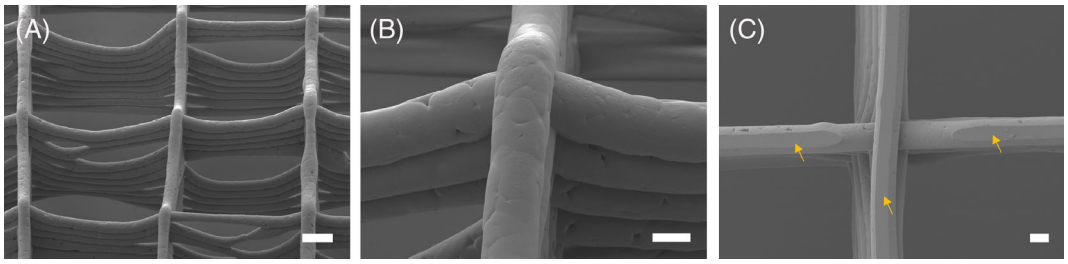

FIGURE 3 SEM images showing (A,B) above- and (C) underneath-views of a scaffold printed at a collector temperature of 110°C and a speed of 4000 mm/min resulting in 20 alternating layers. The yellow arrows in (C) indicate the embossing of the fibers when touching the heated collector. Scale bars are (A) 100 μm and (B,C) 25 μm

smaller distance of 3.3 mm. Furthermore, the differences in the cooling rates/solidification of the jet are leading to a change in the fiber morphology with increasing collector temperature. Fibers with spherulites can be seen starting at a collector temperature of around 100°C (Figure 1). Similar observations have been reported when MEW-processing polypropylene using a heated collector.[16]

At collector temperature of 150°C, the processed fibers lose their roundish shape as well as the uniformity of the resulting strands. The collector distance was also further reduced to around 2.5 mm to process straight fibers. Furthermore, the cooling of the jet is not fast enough resulting in flattening of each fiber. The individual layers are still visible, nevertheless, the stacked fibers start to form a more solid-like wall. Therefore, a collector temperature of 150°C was defined as the maximum, as the fibers significantly flatten resulting in an increase in fiber diameter and a less roundish fiber shape.

The maximum number of layers stacked upon each other was either limited due to the lifting of the scaffold, which was reduced using higher collector temperatures but was still present, or due to the heat of the print head getting too hot/close to the uppermost layer (Figure 2D and Figure S4). It was observed that increasing collector temperatures allowed an increasing number of stackable layers up to a collector temperature of 100–120°C resulting in 20 alternating layers due to the inhibiting warping phenomenon.

However, with increasing number of layers, the height of the constructs increases as well, leading to a decrease in distance between the deposited fiber and the heated print head. This caused melting of the uppermost layer and resulted in "spheres" appearing at the top of the scaffold, as shown in Figure 2D and in Video S2. While these are the result of an unintended artifact—the excessive heating due to the proximity of the MEW head, the regularity and size of the spheres (206 ± 52 μm) may offer possibilities for certain applications and introduce a clear anisotropy between the top and bottom of the scaffold. Figure 2E summarizes how the maximum number of well-formed layers are affected by the collector temperature.

With respect to utility of these structures on the scaffold, it was investigated for any possible super hydrophobicity in regard to similarities to favorable air-grid surface patterning[20,21] and biomimetic structures.[22] The water contact angles of the processed scaffolds were measured to have a maximum average value of 134 ± 5°for a scaffold with a 250 μm fiber spacing printed with a 30G nozzle and a collector to print head distance of around 2.5 mm (Figure S5).This did not indicate a substantially higher contact angle over flat substrates, with results further summarized in Table S1. Similar contact angles, in the range of 136° to 153°, have been shown in literature for SESmembranes.[14,23]

When balancing the decrease in the warping phenomenon, as well as sufficient fiber fusion (Figure 1), the focus for the increasing layer stacking will be on the collector temperatures at 110°C and 120°C. Scaffolds printed at these collector temperatures and a printing speed of 4000 mm/min resulted in well-stacked layers with up to 10 layers in *x*- and *y*-direction meaning a total of 20 alternating layers, as shown in Figure 3.

The most promising results to enhance the printability of PVDF were achieved with a collector temperature of 110°C. The amount of layers was increased from previous results[5] printing five layers in each *x*- and *y*-direction to up to 10 layers in *x*- and *y*-direction. The resulting fibers already show spherulites on their surface similar to the scaffolds printed at a collector temperature of 150°C (Figure 1). Furthermore, the layers are well stacked on top of each other, however, due to the heat between the collector and the print head and the resulting reduced solidification, some of the fibers are sagging in-between the crossing points of the box structure. Even though the lifting and warping of the printed constructs was decreased, it was not achievable to completely prevent this phenomenon from occurring.

The maximum scaffold height using PVDF is ultimately limited by the decreasing distance between the uppermost layer and the print head. As discussed in a previous review,[3] the drawback of MEW regarding the lack of a wide variety of MEW-processable materials, as well as the freedom in design, is quite often limited by the printer design and features. Using a MEW printer with an adjustable Z-height and adjustable high voltage while printing would potentially help to overcome the before mentioned boundary in the layer stacking height, as previously shown.[7] Furthermore, the thermal gradient of the jet[24] would be better defined within a controlled temperature/humidity environment to tailor fiber fusion.

4 | CONCLUSION

In this study, the use of a heated collector enabled the increase inprintable layers for PVDF. The heat improved the attachment of the

first layers to the collector substrate and successfully decreased the lifting and warping effect. Furthermore, the formation of coalesced spheres appeared at the fiber intersections at collector temperatures of 150°C that might have some potential utility in scaffold design. Future work should be performed using dynamic printing conditions with both, collector distance and voltage, changing during MEW-processing to control the print and even adjusting the collector temperature during printing. This should control the fiber fusion and solidification rates and allow much thicker samples to be fabricated via MEW.

ACKNOWLEDGMENTS

We gratefully acknowledge financial support by the Volkswagen Foundation (grant number 93418) and additionally Juliane C. Kade is supported by the Joachim Herz Foundation. The video editing by Dr. Ievgenii Liashenko and the technical assistance of Dr. Philipp Stahlhut for SEM imaging is appreciated while the Zeiss Crossbeam CB 340 SEM was funded by the German Research Foundation (DFG) State Major Instrumentation Programme (INST 105022/58-1 FUGG). We also thank Andreas Züge for his input and assistance with recording videos.

DATA AVAILABILITY STATEMENT

The data that support the findings of this study are available from the corresponding author upon reasonable request

ORCID

Robert Luxenhofer https://orcid.org/0000-0001-5567-7404
Paul D. Dalton https://orcid.org/0000-0001-9602-4151

REFERENCES

1. Robinson TM, Hutmacher DW, Dalton PD. The next frontier in melt electrospinning: taming the jet. *Adv Funct Mater*. 2019;29(44):1904664.
2. Hochleitner G, Jungst T, Brown TD, et al. Additive manufacturing of scaffolds with sub-micron filaments via melt electrospinning writing. *Biofabrication*. 2015;7(3):035002.
3. Kade JC, Dalton PD. Polymers for melt electrowriting. *Adv Healthc Mater*. 2021;10(1):2001232.
4. Wunner FM, Wille ML, Noonan TG, et al. Melt electrospinning writing of highly ordered large volume scaffold architectures. *Adv Mater*. 2018;30(20):e1706570.
5. Florczak S, Lorson T, Zheng T, et al. Melt electrowriting of electroactive poly(vinylidene difluoride) fibers. *Polym Int*. 2018;68(4):735-745.
6. Luo Z, Chen J, Zhu Z, et al. High-resolution and high-sensitivity flexible capacitive pressure sensors enhanced by a transferable electrode array and a micropillar–PVDF film. *ACS Appl Mater Interfaces*. 2021;13(6):7635-7649.
7. Pramod K, Gangineni RB. Low voltage bipolar resistive switching in self-assembled PVDF nanodot network in capacitor like structures on Au/Cr/Si with Hg as a top electrode. *Org Electron*. 2017;42:47-51.
8. Lee JP, Lee JW, Baik JM. The progress of PVDF as a functional material for triboelectric nanogenerators and self-powered sensors. *Micromachines*. 2018;9(10):532.
9. Wang X, Sun F, Yin G, Wang Y, Liu B, Dong M. Tactile-sensing based on flexible PVDF nanofibers via electrospinning: a review. *Sensors*. 2018;18(2):330.
10. Bae J-H, Chang S-H. PVDF-based ferroelectric polymers and dielectric elastomers for sensor and actuator applications: a review. *Funct Compos Struct*. 2019;1(1):012003.
11. Li Y, Liao C, Tjong SC. Electrospun polyvinylidene fluoride-based fibrous scaffolds with piezoelectric characteristics for bone and neural tissue engineering. *Nanomaterials*. 2019;9(7):952.
12. Munirasu S, Banat F, Durrani AA, Haija MA. Intrinsically superhydrophobic PVDF membrane by phase inversion for membrane distillation. *Desalination*. 2017;417:77-86.
13. Wu J, Ding Y, Wang J, et al. Facile fabrication of nanofiber- and micro/nanosphere-coordinated PVDF membrane with ultrahigh permeability of viscous water-in-oil emulsions. *J Mater Chem A*. 2018;6(16):7014-7020.
14. Liao Y, Wang R, Tian M, Qiu C, Fane AG. Fabrication of polyvinylidene fluoride (PVDF) nanofiber membranes by electro-spinning for direct contact membrane distillation. *J Membr Sci*. 2013;425-426:30-39.
15. Hrynevich A, Elci BS, Haigh JN, et al. Dimension-based design of melt electrowritten scaffolds. *Small*. 2018;14(22):e1800232.
16. Haigh JN, Dargaville TR, Dalton PD. Additive manufacturing with polypropylene microfibers. *Mater Sci Eng C*. 2017;77:883-887.
17. Alsoufi MS, Elsayed A. Warping deformation of desktop 3D printed parts manufactured by open source fused deposition modeling (FDM) system. *Int J Mech Mechatron Eng*. 2017;17(4):7-16.
18. Kade JC, Tandon B, Weichhold J, et al. Melt electrowriting of poly(vinylidene fluoride-co-trifluoroethylene). *Polym Int*. 2021. https://doi.org/10.1002/pi.6272.
19. Blum C, Weichhold J, Hochleitner G, et al. Controlling topography and crystallinity of melt electrowritten poly(ε-caprolactone) fibers. *3D Print Addit Manufac*. 2021;0(0): null.
20. Chen L, Yang G, Wang S. Air-grid surface patterning provided by superhydrophobic surfaces. *Small*. 2012;8(7):962-965.
21. Kwon Y, Patankar N, Choi J, Lee J. Design of surface hierarchy for extreme hydrophobicity. *Langmuir*. 2009;25(11):6129-6136.
22. Yan YY, Gao N, Barthlott W. Mimicking natural superhydrophobic surfaces and grasping the wetting process: a review on recent progress in preparing superhydrophobic surfaces. *Adv Colloid Interface Sci*. 2011;169(2):80-105.
23. Zhou Z, Wu X-F. Electrospinning superhydrophobic–superoleophilic fibrous PVDF membranes for high-efficiency water–oil separation. *Mater Lett*. 2015;160:423-427.
24. Kade JC, Dalton PD. Polymers for melt Electrowriting. *Adv Healthc Mater*. 2021;10(1):e2001232.

SUPPORTING INFORMATION

Additional supporting information may be found online in the Supporting Information section at the end of this article.

How to cite this article: Kade JC, Otto PF, Luxenhofer R, Dalton PD. Melt electrowriting of poly(vinylidene difluoride) using a heated collector. *Polym Adv Technol*. 2021;32(12):4951-4955. https://doi.org/10.1002/pat.5463